Chapter 2 The Galactic Magnetic Field

2.1 Galactic Dynamo Theory

The galactic disk consists of warm gas, interspersed by cold clouds and hot bubbles. Hot bubbles result from local heating (e.g. OB associations and supernova and super bubble explosions) and eject hot gas into the halo (galactic fountains). These violent motions, in addition to stellar winds, help to drive the turbulence. We believed that these are several mechanisms generate the galactic magnetic field. For examples, the large scale field tangling by turbulence effects of the interstellar matter and from Parker and thermal instabilities, shock waves from supernova remnants and stellar winds and the small scale dynamo (self-generation of random magnetic fields by turbulence of charge particles).

Certainly, all mechanisms act together, the magnetic field is concentrated. In spiral disk, the interstellar gas is compressed when it overtakes the density wave such that the density ratio in the arm to interarm region is approximately 5 : 1 (Robert & Yuan 1970). The magnetic field, being tied to the gas because of the relatively high conductivity of the interstellar medium, will be compressed in the same ratio.

2.2 Regular and Irregular Field

Over the galaxy as a whole the magnetic field can be decomposed into two components: a regular and an irregular component. The regular component is parallel to the spiral arms and depends on distances from galactic plane (z) that is shown in Figure 2.1. Its decrease rather quickly for small z but has a long flat tail for large z.

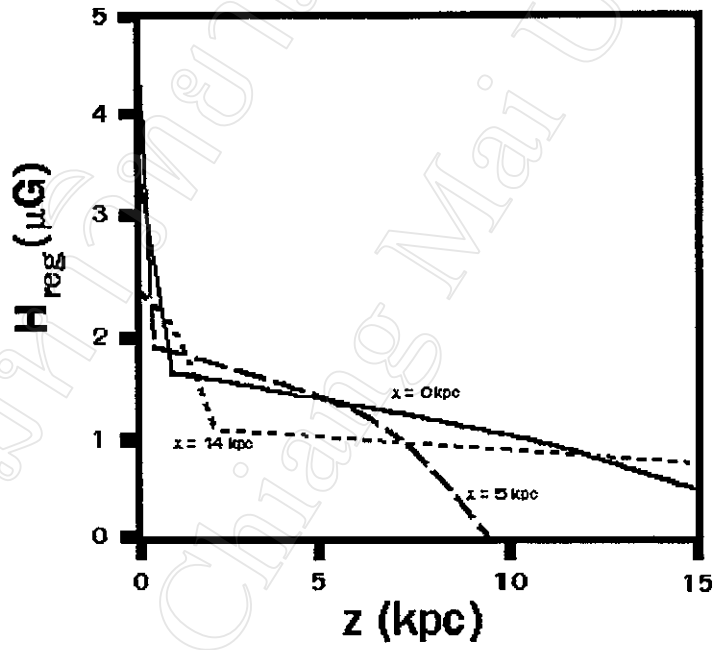

Figure 2.1 The dependence of the regular magnetic field H_{reg} on the distance from the galactic plane at three distances from the galactic center.

The dependence of regular field in the plane passing through the Sun and the galactic center at several distances z is presented in Figure 2.2. The spiral structure vanishes for $| z | > 0.5$ kpc, but for lower $| z |$ the field in the arms reaches quite large values.

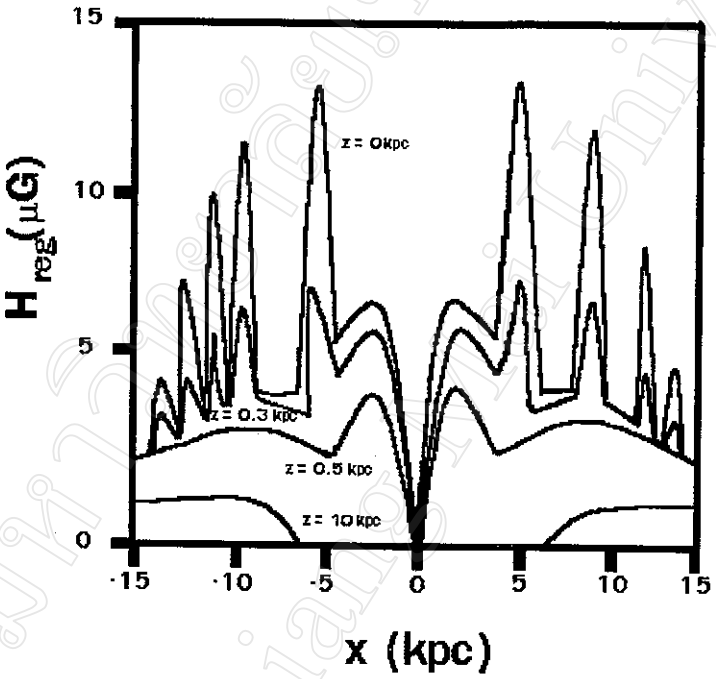

Figure 2.2 The regular magnetic field H_{reg} is shown in the plane perpendicular to the galactic plane, passing through the Sun and the galactic plane at several distances z from the plane.

Due to the compression of the frozen in the field as the density wave acts on the interstellar gas, the irregular magnetic field component was generated by supernova explosions and stellar winds of young O and B type stars. Irregular field component can interpret as due to the superposition of an isotropically random field of approximately equal magnitude (Osborne, Roberts & Wolfendale 1973). Manchester (1974) took the pulsars' s rotation measures of the best-fit residuals as being the strength of random field. This method is equivalent to assuming that the random field is essentially correlated along the path to each pulsar, which is clearly an unreasonable assumption. The magnitude of the regular component is assumed to be a constant factor F times that of the random component through out the galaxy. To account for H_{irreg} , its direction being chosen randomly from an isotopic distribution.

$$F = \frac{H_{reg}}{H_{irreg}} \tag{2.1}$$

Broadbent et al showed that the F ratio is 0.66.

2.3 Compression Profile

The compression profile of density across the arm with a sharp rise on the inner edge followed by approximately exponential decrease is predicted for the two-armed spiral shock. At the position of the Sun, the

compression profile has a modulation of the mean density that can be represented approximately by

$$\rho_c = 4.1 * \exp\left(-13.7\frac{\alpha}{A}\right) + 0.7 \qquad (2.2)$$

Where ρ_c is the ratio of the density of gas at a certain point to the density that it would have in the uncompressed state, A is the radial separation of the two arms adjacent to the point being considered and α is the distance to the inner of the arms. The compression profile widens and becomes less sharply peaked as the galactic distance increases beyond the position of the Sun. For the galactic distance is less than the Sun, the compression profile is only slightly more strongly peaked.

As an alternative Robert and Hausman (1984) assumes that each cloud was a particle in an N-body system orbiting the galactic center and undergoing inelastic collisions with other clouds. The collision between the clouds is assumed to be the dominant star formation mechanism. Modeling shows that galaxy-wide shocks formed and the clouds became concentrated in the spiral arm. By assuming that the width of the arm is the number of degrees between the first points either side of the peak where the density is equal to the average cloud density and taking this to be equivalent to 1 kpc in distance, Broadbent calculated the Gaussian function to fit with the profile of the variation of number density of

clouds with spiral phase at a galactocentric radius of 8 kpc as shown in Figure 2.3.

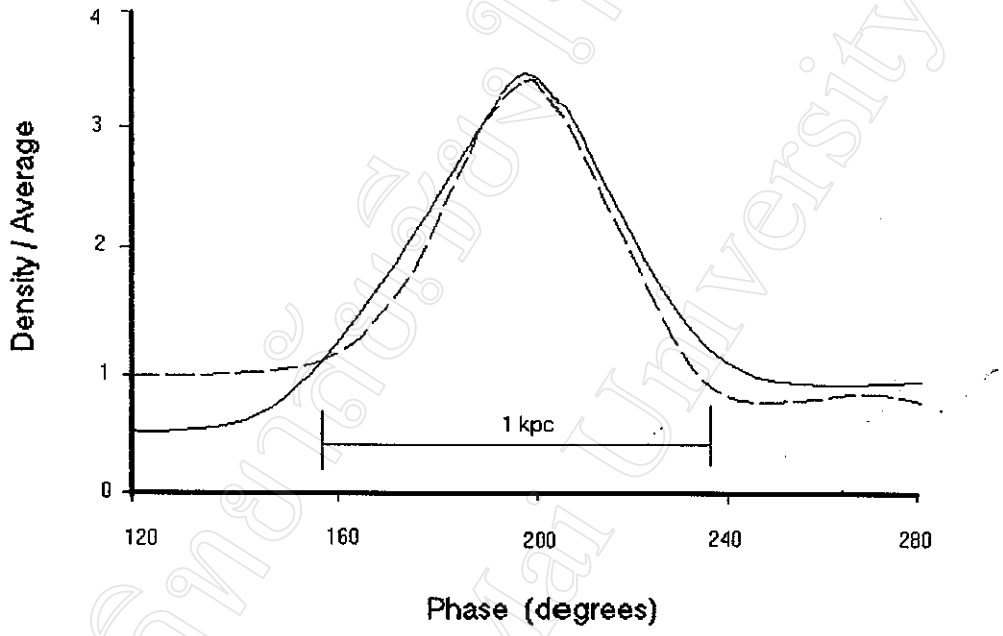

Figure 2.3 The density of clouds is expressed relative to the average and marked underneath the curve is the full width of the arm amounting to the linear distance of 1 kpc. The solid line shows the variation of gas cloud density with phase across a spiral arm at 8 kpc by Robert and Hausman (1984). The dash line is a Gaussian fit and has $\sigma = 0.207$ kpc.

The Gaussian function has a peak values of 2.5, implying that the maximum compression is 3 . 5 : 1 and $\sigma = 0.207$ kpc. Hence, ρ_c after rescaling to the galactic distance of the Sun of 8.5 kpc can be written in the form:

$$\rho_c = CR \cdot f(z) \cdot \exp\left(\frac{-0.5\alpha^2}{0.031}\right) + 1 \tag{2.3}$$

$$CR = \begin{cases} 2.5 & ; \quad 8.5\,kpc \le R \\ (12.75 - R) \cdot 0.5 & ; \quad 8.5\,kpc \le R \le 12.75\,kpc \end{cases} \tag{2.4}$$

Where α is the distance to the nearest arm, inner or outer and the term *f(z)* accounts for the variation of compression of the field with distance, *z* from the plane.

The magnetic field increases the effective square dispersion speed of the gas and damps down the compression in the density waves, i.e. the forcing mechanism for the density wave has to overcome an extra pressure. If, as the latitude variation of the synchrotron radiation indicates, the scale height of the magnetic field is considerably greater than that of the gas, the damping effect of the field on the compression will increase rapidly with *z*. The result of a simple calculation of this effect, due to Brindle et al., which does not pretend to be an accurate quantitative description, is as follows. If one assumes that the magnetic field, the sound speed, C_S and the velocity of entry into the shock, U are all constant for heights above the plane up to several hundred parsecs the strength of the shock is given by

$$\frac{\left\{\left[\left(5V_A^2+6C_S^2+2U^2\right)^2+32U^2V_A^2\right]^{\frac{1}{2}}-\left(5V_A^2+6C_S^2+2U^2\right)\right\}}{2V_A^2}$$

The Alfvén velocity, V_A increases with z and the gas density decreases. Taking H_{reg} = 3 μG for the uncompressed field, U = 35 km/s, C_S = 7 km/s and the variation of gas density of Schmidt (1956), the compression will be reduced to a half at z = 204 pc and is essentially zero beyond 425 pc. For ease of calculation the following polynomial has been fitted to *f(z)*, the damping factor by which the compression in the plane should be multiplied.

$$f(z)=\begin{cases}1+0.908z-23.529z^2+37.35z^3 & ;\quad z\le 0.425\ kpc\\ 0 & ;\quad z\ge 0.425\ kpc\end{cases} \qquad (2.5)$$

2.4 Synchrotron Radiation

Particles accelerated by a magnetic field, H will radiate. For relativistic particles, the frequency spectrum is much more complex and can extend to many times the gyration frequency. The radiation is known as synchrotron radiation. Simultaneously, the observed radiation is concentrated within the cone of emission of angular width $1/\gamma$ includes the direction of observation, where γ is the Lorentz factor.

The intensities of electric and magnetic fields can be computed from the Lienard-Wiechert potentials.

$$\vec{E} = -\frac{1}{c}\frac{\partial}{\partial t}\vec{A} - \vec{\nabla}\phi$$
$$\vec{H} = \vec{\nabla} \times \vec{A} \tag{2.6}$$

The power emitted by particle within a narrow cone at a frequency ν, $P(\nu)$

$$P(\upsilon) = \frac{\sqrt{3}e^3}{mc^2} H_{\perp} \left[\frac{\upsilon}{\upsilon_c} \int_{\frac{\upsilon}{\upsilon_c}}^{\infty} K_{\frac{5}{3}}(\xi) d\xi \right] \tag{2.7}$$

Where $K_{5/3}(\xi)$ is a modified Bessel function and the shape of the quantity in square brackets is shown in Figure 2.4.

The peak of $F(x)$ or the maximum synchrotron emission is relative to the critical frequency, ν_c

$$F(x) = x \int_{\frac{\upsilon}{\upsilon_c}}^{\infty} K_{\frac{5}{3}}(\xi) d\xi \qquad ; \quad x = \frac{\upsilon}{\upsilon_c} \tag{2.8}$$

$$\upsilon_c = \frac{3e}{4\pi m^2 c^5} H_{\perp} E^2 \tag{2.9}$$

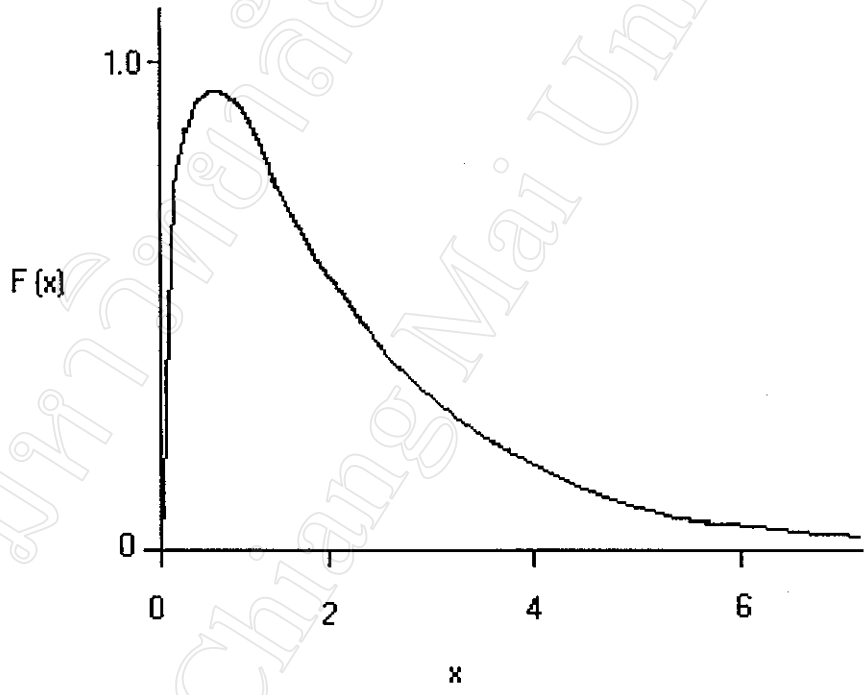

Figure 2.4 The synchrotron spectrum from a single electron as a function of $x = \nu/\nu_c$ *where* ν_c *is the synchrotron critical frequency.*

For $H_{\perp}$ is the magnetic field component perpendicular to the direction of the electron velocity, v. when the angle between v and H is θ,

$$H_{\perp} = H \sin\theta \tag{2.10}$$

When synchrotron radiation coming from a stationary region with the uniform distribution of electron in vacuum, the emission coefficient, ε_{ν}

$$\varepsilon_{\upsilon} = \int_{0}^{2\pi}\int_{0}^{\infty} N(E)\,P(E)\,dE \tag{2.11}$$

Often the number density of electrons, with energies between E and $E+dE$, $N(E)$ can be approximately expressed by a power-law distribution of relativistic electrons.

$$N(E)dE = N_e E^{-\alpha} dE \tag{2.12}$$

Therefore, the source function, the accumulated intensity of radiation through in the line of sight at frequency ν, S_{ν}

$$S_\upsilon = \frac{1}{4\pi}\int_0^S\int_0^\infty N_e E^{-\alpha} P(\upsilon)\,dE\,ds$$

$$= \frac{\sqrt{3}e^3}{4\pi mc^2}\int_0^S H_\perp N_e \int_0^\infty E^{-\alpha}\,\frac{\upsilon}{\upsilon_c}\int_{\frac{\upsilon}{\upsilon_c}}^\infty K_{\frac{5}{3}}(\xi)\,d\xi\,dE\,ds$$

$$= \frac{\sqrt{3}e^3}{8\pi mc^2}\left(\frac{3e}{4\pi m^3c^5}\right)^{\frac{\alpha-1}{2}}\int_0^S N_e \frac{H_\perp^{\frac{\alpha+1}{2}}}{\upsilon^{\frac{\alpha-1}{2}}}\int_0^\infty x^{\frac{\alpha-1}{2}}\int_x^\infty K_{\frac{5}{3}}(\xi)\,d\xi\,dx\,ds \qquad (2.13)$$

Because the emission is non-thermal, we now assume by the Rayleigh-Jeans limit, $h\nu << kT$ and under the Local Temperature Equilibrium,

$$S_\upsilon \cong \frac{2kT_b\upsilon^2}{c^2} \qquad (2.14)$$

The observed Brightness Temperature, T_b

$$T_b = \frac{\sqrt{3}e^2}{16\pi km}\left(\frac{3e}{4\pi m^3 c^5}\right)^{\frac{\alpha-1}{2}} \int_0^S N_e \frac{H_\perp^{\frac{\alpha+1}{2}}}{\upsilon^{\frac{\alpha+3}{2}}} \int_0^\infty x^{\frac{\alpha-1}{2}} \int_x^\infty K_{\frac{5}{3}}(\xi)\, d\xi\, dx\, ds$$

$$= \frac{\sqrt{3}e^2}{16\pi km}\left(\frac{3e}{4\pi m^3 c^5}\right)^{\frac{\alpha-1}{2}} \int_0^S N_e \frac{H_\perp^{\frac{\alpha+1}{2}}}{\upsilon^{\frac{\alpha+3}{2}}} \Gamma\left[\frac{3\alpha-1}{12}\right]\Gamma\left[\frac{3\alpha+7}{12}\right]\Gamma\left[\frac{\alpha+\frac{7}{3}}{\alpha+1}\right] ds \qquad (2.15)$$

By the summary spectrum of Meyer (1974), French & Osborne (1976) obtain the parameter $\alpha = 2.6$, then

$$T_b = 6.168 \times 10^4\, \upsilon^{-2.8} \int_0^S N_e H_\perp^{1.8}\, ds \qquad (2.16)$$

Now, we can see that the brightness temperature depends on the electron density $N_e(s)$ and the perpendicular component of the magnetic field $H_\perp(s)$ as a function of distance, s, along the line of sight.

As discussed below, the magnetic field can be considered to have two components, a regular component whose direction lies along the spiral arms, parallel to the galactic plane, and an irregular component. It was assumed that the overall distribution of orientation of the latter is

isotropic. This means that, to a good approximation, above equation can be rewritten as

$$T_b = 6.168\times10^4\, \upsilon^{-2.8} \int_0^S N_e(s)\left[H_{\perp reg}(s) + H_{\perp irreg}(s)\right]^{1.8} ds \qquad (2.17)$$

French (1977) showed that equation (2.17) can be approximately written in the form:

$$T_b = 6.168\times10^4\, \upsilon^{-2.8} \int_0^S \left[N_e(s) H_{\perp reg}(s)^{1.8} + N_e(s) H_{\perp irreg}(s)^{1.8}\right] ds \qquad (2.18)$$

We assume that the ratio of the regular and irregular field, F, is constant over the galaxy in the interarm regions but in the arms one would expect it to change. In the absence of any other effects one would expect the irregular component to undergo a certain degree of alignment along the direction of the arm, the extent of which depends on the compression in the arm. French calculated the effective component of the regular field perpendicular to the line of sight in terms of the regular component, the compression ratio, F, of the regular to irregular to irregular field in the uncompressed state. The equation (2.18) then become:

$$T_b = 6.168\times10^4\,\upsilon^{-2.8}\int_0^S\left[N_e(s)\left(\rho_c(s)H_{reg}(s)\sin\theta\right)^{1.8} + 0.6861N_e(s)\left(\frac{\rho_c(s)H_{reg}(s)}{F}\right)^{1.8}Y(s)\right]ds \tag{2.19}$$

where

$$Y(s) = 1 - 0.477\left(\frac{\rho_c^2 - 1}{\rho_c^2}\right)\cdot\cos^2\theta \tag{2.20}$$

It has been assumed that the variation of H_{reg} is independent of z and all variations in that direction are included in the electron density and the demodulation of the compression factor, ρ_c, in a spiral arm.

2.5 Distribution of Cosmic Ray Electron Density

In equation (2.19) the high energy cosmic ray (CR) electrons, of energy E GeV, which are accelerated by the magnetic field are assumed to have a power law differential intensity spectrum:

$$Flux = N_e(s)E^{-2.6}dE \qquad m^{-2}sr^{-1}s^{-1} \tag{2.21}$$

Initially, to simplify the parameterization, the electron density is assumed to have no radial dependence within the plane of the galaxy. All the variation of emissivity is assigned to the overall radial dependence of the galactic magnetic field and its modulation by the presence of a spiral arm. We therefore assign the locally measured value to N_e. In the earlier Durham models it was taken that $N_e = 80^{+70}_{-30}$ $m^{-2}sr^{-1}s^{-1}GeV^{-1}$ from a review by Meyer (1974). Since then there have been increase in the size of the *CR* electron detectors and in their ability to discriminate against the *CR* nuclear background, which has about two orders of magnitude higher intensity. A recent measurement was that of Golden et al. (1994) performed in 1989 using a large super-conducting magnet spectrometer and an imaging calorimeter. The flattening in the spectrum below 4 GeV is consistent with the effects of solar modulation. For the production of 408 MHz synchrotron radiation implies that, in a 3 μG field, the electron energy of interest is around 3 GeV. Taking into account the solar modulation, it can be seen that above value of N_e still gives a reasonable representation of the local interstellar intensity.

The assumption that the electron flux density does not vary between the arm and interarm regions requires that the electrons diffuse fast compared with the speed of the rotation of the density wave. The density wave takes ~ 3 x 10^7 years to pass a given point. Measurements of the age of *CR* nuclei in the galactic disk indicate that they diffuse with a diffusion coefficient ~ 3 x 10^{28} cm^2s^{-2} and those *CR* electrons, if they propagate in the same way, therefore diffuse ~ 2 kpc in this time. This is sufficient to move freely from the arm to the interarm region or vice versa. Although in the plane the electron flux density is taken to be the

same everywhere, out of the plane one would expect there to be a decrease with height above the plane due to diffusive escape of electrons from the galaxy. In our parameterization of the synchrotron emissivity distribution we assign essentially all of the variation with z, the distance from the galactic plane to the variation in the electron flux. The exception to this is the decrease in modulation of the magnetic field strength due to compression in the spiral arms with height above the plane.

Phillipps et al. (1981b) in the derivation of a 3-dimensional model of the emissivity distribution by the unfolding technique obtained the following polynomial expression for the z-dependence of N_e when $R_{SUN} = 10$ kpc.

These represents a 'thick disk' surrounded by an extensive, low emissivity 'halo'. The synchrotron-emitting halo does not, however, have the quasi-spherical shape that is normally assumed for the material halo. Such a spherical form would result in higher brightness temperatures at $|b| \sim 45°$ towards the inner part of the galaxy than is observed. Instead they adapted that the halo and thick disk mirror the thinner gaseous disk in having a scale height that decrease towards the galactic center. The above expression therefore contains an R-dependent scaling factor, z_0, normalized to unit at R_{SUN}:

$$N_e\left(\frac{z}{z_0}\right)=80x\begin{cases}1.063+0.9344\left(\frac{z}{z_0}\right)-3.551\left(\frac{z}{z_0}\right)^2+ & \\ 2.645\left(\frac{z}{z_0}\right)^3-0.8192\left(\frac{z}{z_0}\right)^4+ & \\ 0.1134\left(\frac{z}{z_0}\right)^5-0.00579\left(\frac{z}{z_0}\right)^6 & \left(\frac{z}{z_0}\right)\le 1.1 \\ 0.30788-0.01844\left(\frac{z}{z_0}\right) & 1.1\le\left(\frac{z}{z_0}\right)\le 16.7 \\ 0 & \left(\frac{z}{z_0}\right)\ge 16.7\end{cases} \tag{2.22}$$

where

$$z_0=0.591-0.0652R+0.0106R^2 \tag{2.23}$$

However this polynomial has its maximum value at z/z_0 = 0.15 kpc which leads to a small dip in the latitude profile cut at z = 0. As we go on to investigate the absorption in the plane at low frequencies it is best to remove this artifact in the model. Thus we have modified this from in order to give a flat top by setting N_e = 80 x 1.063 if $z/z_0 < 0.34105$ as seen in Figure 2.5.

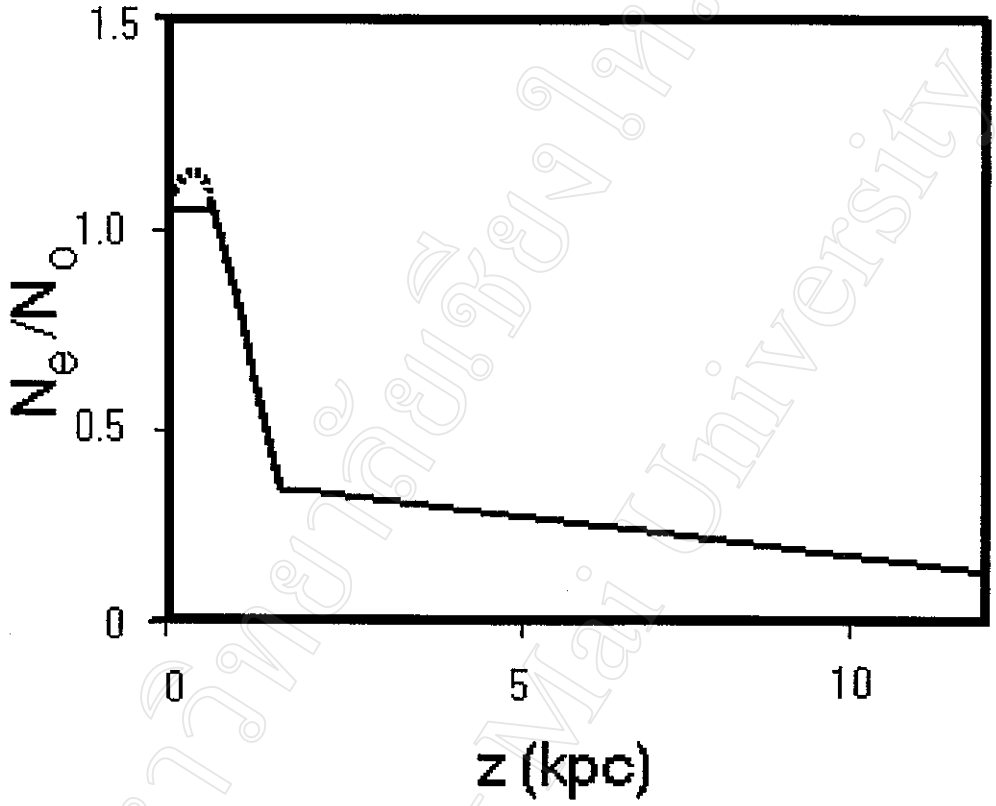

Figure 2.5 The distribution of electron flux density with height above the plane at the solar galactic radius, R_{SUN} = 10 kpc. The dot line uses the equation (2.22). The solid line shows that modifying form of N_e follow as equation (2.24).

This has a significant effect on the fine scale (1/4)° calculation out to $|b|$~1°. For the 408 MHz modeling, Δb was 1° and the data were convolved to 51° HPBW. When this is done with the new model:

1.) The reduction in the convolved $\Delta b = 1°$ profile is too small to see at $b = 0$ therefore it is fitted to the observation very much.

2.) The changes in the latitude profile are < 1% so there is no significant change to the latitude cut fits.

The distribution of electron flux density, with this change and the rescaling to $R_{SUN} = 8.5$ kpc becomes

$$N_e\left(\frac{z}{z_0}\right) = 80x\begin{cases} 1.063 & \left(\frac{z}{z_0}\right) \le 0.2899 \\ 1.063 + 1.099\left(\frac{z}{z_0}\right) - 4.915\left(\frac{z}{z_0}\right)^2 + & \\ 4.307\left(\frac{z}{z_0}\right)^3 - 1.569\left(\frac{z}{z_0}\right)^4 + & \\ 0.256\left(\frac{z}{z_0}\right)^5 - 0.015\left(\frac{z}{z_0}\right)^6 & 0.2899 \le \left(\frac{z}{z_0}\right) \le 0.935 \\ 0.30788 - 0.0217\left(\frac{z}{z_0}\right) & 0.935 \le \left(\frac{z}{z_0}\right) \le 14.195 \\ 0 & \left(\frac{z}{z_0}\right) \ge 14.195 \end{cases} \tag{2.24}$$

where

$$z_0 = 0.591 - 0.0767R + 0.0147R^2 \tag{2.25}$$